arXiv:astro-ph/0001369v1 21 Jan 2000

Accepted for publication in the *Astrophysical Journal*

ON THE DETERMINATION OF STAR FORMATION RATES IN EVOLVING GALAXY POPULATIONS

J. Afonso

Blackett Laboratory, Imperial College, Prince Consort Rd, London SW7 2BW, UK

j.afonso@ic.ac.uk

L. Cram

School of Physics, University of Sydney, Sydney NSW 2006, Australia

l.cram@physics.usyd.edu.au

and

B. Mobasher

Blackett Laboratory, Imperial College, Prince Consort Rd, London SW7 2BW, UK

b.mobasher@ic.ac.uk

ABSTRACT

The redshift dependence of the luminosity density in certain wavebands (e.g. UV and Hα) can be used to infer the history of star formation in the populations of galaxies producing this luminosity. This history is a useful datum in studies of galaxy evolution. It is therefore important to understand the errors that attend the inference of star formation rate densities from luminosity densities. This paper explores the self-consistency of star formation rate diagnostics by reproducing commonly used observational procedures in a model with known galaxy populations, evolutionary histories and spectral emission properties. The study reveals a number of potential sources of error in the diagnostic processes arising from the differential evolution of different galaxy types. We argue that multi-wavelength observations can help to reduce these errors.

Subject headings: cosmology: observations — galaxies: evolution — stars: formation

1. INTRODUCTION

The stellar content and hence the spectral energy distribution (SED) of a galaxy depends on many factors. Accurate predictions of galaxy SEDs require sound theories of stellar evolution and

stellar atmospheres, including transient and extreme phases that remain difficult to model. In addition, the evolution of a galaxy SED depends on (i) the initial mass function (IMF) of stars and (ii) the history of the star formation rate (SFR). Parts of the SED, such as the UV continuum and the Balmer lines, are sensitive to the recent IMF and SFR, while other parts, such as the IR continuum, reflect long-term averages. This opens the possibility of using observations of SEDs to determine the current and past SFR in a particular galaxy, and, by observing the SEDs of populations of galaxies over a range of redshifts, the history of star formation in the universe. To do this, one needs a galaxy spectral synthesis model connecting SEDs with SFRs and IMFs. Early models of this kind were reviewed by Tinsley & Danly (1980), and more recent work is summarised by Leitherer *et al.* (1996) and Schaerer (1999).

The past decade or so has seen the acquisition of a rapidly growing body of data on the distribution, over redshift, absolute luminosity, and galaxy type, of those spectral properties of galaxies sensitive to star formation rates. Particularly notable have been new data on rest-frame UV luminosities to redshifts $z \approx 4$ (Lilly *et al.* 1996; Madau *et al.* 1996; Cowie *et al.* 1997; Connolly *et al.* 1997; Madau, Pozzetti & Dickinson 1998; Pascarelle, Lanzetta & Fernández-Soto 1998; Treyer *et al.* 1998; Cowie, Songaila & Barger 1999; Sullivan et al. 1999), emission line luminosities in Hα and [OII] λ372 nm to $z \approx 1$ (Gallego *et al.* 1995; Cowie *et al.* 1997; Tresse & Maddox 1998; Glazebrook *et al.* 1998), and photometry (with redshift estimates to $z \approx 1$) in the far-IR, sub-mm and radio spectral bands (Rowan-Robinson *et al.* 1997; Flores *et al.* 1999; Hughes *et al.* 1998; Blain *et al.* 1999; Cram *et al.* 1998). The data have been interpreted by several of these authors using galaxy spectral synthesis models, to yield estimates of the star formation rate as a function of redshift.

Although it is widely recognised that there are numerous sources of uncertainty in the process of inferring star formation rates from the observable diagnostics, there have been few systematic, internally consistent investigations of these uncertainties (see also Schaerer 1999). In an attempt to bridge this gap, this paper uses a galaxy spectral evolution code to test the self-consistency of common diagnostic procedures. We do this by comparing the known star formation history of a model universe containing specified galaxy populations with the star formation history that would be inferred by applying commonly adopted diagnostic procedures. Two questions are addressed: (1) are star formation rates derived from Hα and UV luminosities consistent with each other?, and (2) are star formation rates inferred from luminosity densities consistent with the true star formation rate in the model? It is important to stress that we do not aim to explore the validity of any particular model of cosmic star formation history: we are concerned here only with checking the internal consistency of diagnostic procedures.

2. THE MODEL AND ITS CALIBRATION

We use the galaxy spectral evolution model PEGASE (Fioc & Rocca-Volmerange 1997) and the galaxy population evolution model of Pozzetti, Bruzual & Zamorani (1996) to predict the evolution

of the Hα and UV luminosity densities in a "model universe" with a known star formation history. The key steps in our approach are (1) calculate the evolution of the actual SFR density defined by the parameters given in the model; (2) combine PEGASE and the model universe to predict the evolving luminosity densities; (3) use PEGASE to calibrate the SFR in terms of luminosity density using the methods commonly applied to observations, and (4) combine the calibration and the predicted luminosity density evolution to deduce the SFR history for comparison with step (1).

Pozzetti *et al.* (1996) explored pure luminosity evolution (PLE) models based on a mix of four galaxy types, E/S0, Sab-Sbc, Scd-Sdm and very Blue (vB). The different types are denoted hereinafter by the parameter k. The local luminosity function $\Phi_k(L)$ of each type in each selected waveband is parametrised by the local space density Φ_k^*, characteristic luminosity L_k^*, and faint-end slope α_k. Each type also has a characteristic IMF $\Psi_k(M)$ and star formation rate history, $\dot{\rho}_k(t)$. A Scalo-type IMF is used for the E/S0 and Sab-Sbc types, hereinafter called "early", while a Salpeter-type IMF is used for the Scd-Sdm and vB types, hereinafter called "late". For the E/S0 galaxies, Pozzetti *et al.* consider two models distinguished by different e-folding times (τ_1, τ_2) in their SFR. We adopt the τ_2 model.

Pozzetti *et al.* (1996) constructed their model universe to match a number of observational constraints, including the source count distribution in several optical and IR photometric bands, the distribution of colours as a function of apparent magnitude, and the distribution of redshifts as a function of magnitude. Pozzetti *et al.* (1996) exhibit a PLE model which, in an $\Omega = 0$ Friedmann cosmology, leads to acceptable agreement with almost all of these constraints. They also deduce that PLE models in a flat ($\Omega = 1$) cosmology cannot reproduce several aspects of the data, and therefore we consider only the $\Omega = 0$ and $H_0 = 50$ km s^{-1} Mpc^{-1} model.

One constraint not used by Pozzetti *et al.* is the observed redshift dependence of the luminosity density in certain wavebands. Figure 1 compares the UV luminosity density ($\mathcal{L}^{200}$ – see below) of the model of Pozzetti *et al.* with the observations of Cowie, Songaila & Barger (1999). While there remain significant uncertainties in the measured UV luminosity density (cf. Lilly *et al.* 1996; Cowie, Songaila & Barger 1999; Sullivan et al. 1999), there is satisfactory agreement between the prediction and recent measurements. The significance of this will be amplified below.

Our application of PEGASE takes place in two steps. First, for galaxies of type k we compute the time-dependent spectral emission which follows the instantaneous formation of 1 $M_\odot$ of stars. We use the evolutionary tracks of Bressan *et al.* (1993) supplemented to later evolutionary phases and to lower masses as indicated in Fioc & Rocca-Volmerange (1997). We use the spectral stellar library described by Fioc & Rocca-Volmerange (1997). We ignore extinction in the prediction of the UV luminosity, and assume the number of ionizing photons to be 70% of the Lyman continuum photons. To ensure agreement with the evolutionary tracks, PEGASE has an upper limit of 120 $M_\odot$ for the chosen IMFs. This leads to a minor inconsistency with the upper limit of 125 $M_\odot$ used by Pozzetti *et al.*, but this has no effect on our conclusions.

In the second step we convolve the time-dependent spectral emission with the star formation

rate history $\dot{\rho}_k(t)$, to determine the evolution of L^*_k. Inserted into the luminosity function in the model of Pozzetti *et al.* this yields a prediction of the luminosity density $\mathcal{L}^p_k(t)$ produced in the (rest-frame) waveband p at time t by the population k undergoing star formation with a rate density of $\dot{\rho}_k(t)$. The total SFR density is then clearly

$$\dot{\rho}(t) = \sum_k \dot{\rho}_k(t),$$

and the total luminosity density in waveband p is

$$\mathcal{L}^p(t) = \sum_k \mathcal{L}^p_k(t).$$

For illustration it is convenient to define the ratio

$$R^p_k(t) = \dot{\rho}_k(t)/\mathcal{L}^p_k(t).$$

It is also convenient to define a global ratio for waveband p as

$$R^p(t) = \dot{\rho}(t)/\mathcal{L}^p(t).$$

Our notation recognises that R may be time dependent, and may depend on the galaxy type k and waveband p.

Figures 2(a) and (b) exhibit the evolution with time of $R^p_k(t)$ for each galaxy type and of the global ratio $R^p(t)$, respectively for the 200 nm continuum and for Hα. As previously stressed by Kennicutt (1983), Schaerer (1999) and others, the ratio for Hα in each galaxy type rapidly settles to a steady value, reflecting the fact that Hα emission is completely controlled by the short-lived, massive component of the IMF. The difference of ≈ 0.5 dex between the asymptotic ratios for the early and late-type galaxies is due to the adoption of Scalo and Salpeter IMFs, respectively, for the two types.

The evolution of $R^p_k(t)$ for the 200 nm continuum is quite complex. For the E/S0 type, in which most star formation takes place in the first 2 Gyr, the ratio displays a steady decline over ≈ 1 Gyr, a plateau to ≈ 8 Gyr, and a subsequent decline to the present epoch. The initial decline arises from the rapid evolution of the initial burst, while the later decline reflects the late stages of evolution of relatively low mass stars at a time when few new stars are being born. The extended plateaux in the Sab-Sbc and Scd-Sdm types reflect the slower change in the star formation rate in these populations, while the difference in asymptotic value is due to the different IMFs. By definition, the vB component has a ratio equal to that of the Scd-Sdm type at an age of 100 Myr.

To emulate observational procedures, we require calibration constants C^p that do not depend on time or galaxy type. These have been estimated by previous workers using galaxy spectral synthesis models over a range of star-forming histories and ages, and selecting a "typical" value (e.g. Kennicutt, Tamblyn & Congdon 1994; Schaerer 1999). We have conducted a similar study using PEGASE. As with previous derivations of calibration factors, we find a significant sensitivity

to the IMF, but this is not the focus of our study. Accordingly, we explore calibrations based on both the Salpeter ("late") and Scalo ("early") models adopted by Pozzetti *et al.* The calibration constants are listed in Table 1. We acknowledge that there is inevitable uncertainty in the precise numerical values of the calibration factors in our study, as there is in other studies, but stress that this uncertainty has no effect on our conclusions.

3. THE INFERRED STAR FORMATION RATE AND ITS EVOLUTION

Figure 3 exhibits the time dependent star formation rate density of each galaxy type, and for the totality of the populations. Early-type galaxies dominate star formation for $z > 1$, while all types except E/S0 contribute for $z \approx 0$. Figure 4 shows the global star formation history that would be inferred from the luminosity densities using each of the calibration factors listed in Table 1. Despite the self-consistency in our approach, in no case does the inferred value match the actual star formation history shown as the solid line in Figures 3 and 4.

There are two reasons for the discrepancies seen in Figure 4 at $z = 0$. First, the fact that the early and late-type populations have different IMFs implies that neither a Salpeter nor a Scalo calibration factor applied to the global luminosity density will yield the true star formation rate. Secondly, even in the absence of this difference, the 200 nm and Hα calibrations are not consistent because they refer to different averages over the recent star formation history. This can be seen clearly in Figure 2, where the vB and Scd-Sdm components have identical values of $R_k^{\mathrm{H}\alpha}(t)$ after the initial transient phase of ≈ 10 Myr, but have different values of $R_k^{200}(t)$ except at 100 Myr.

Another way to view the discrepancy is to contrast the relative contribution of each galaxy type to the luminosity density with its contribution to the star formation rate. Table 2 shows, for example, that at $z = 0$ the vB galaxy type contributes 32% to $\mathcal{L}^{\mathrm{H}\alpha}$ and 27% to $\mathcal{L}^{200}$, while its contribution to the star formation rate itself is 24%.

At high redshift yet another factor comes into play: the relative mix of galaxy types changes as each undergoes luminosity evolution with its specified star formation history. The systematic errors seen at $z = 0$ therefore change with redshift. Not surprisingly, we see that for each waveband the Scalo IMF calibration is poorer than the Salpeter at $z = 0$, and that the situation reverses at $z = 2$, since the early-type galaxies become dominant at higher redshifts. There are, however, always systematic errors in the inferred star formation rates.

4. DISCUSSION AND PROSPECTS

The qualitative trends in our results could have been anticipated on the basis of previous studies of the influence of the IMF and the star formation history on the calibration of luminosity densities in terms of star formation rates (e.g. Schaerer 1999). Our study shows quantitatively that

attempts to infer the SFR density locally and over a range of redshifts can be compromised by the presence of different galaxy types, whose mix evolves differentially. Such differential evolution is an almost inevitable consequence of models based on pure luminosity evolution or, indeed, other descriptions of cosmic evolution. Insofar as the model of Pozzetti *et al.* (1996) is typical in respect of its mixture of galaxy types, systematic errors can be anticipated of the order of a factor of at least 2 in both the absolute value of SFR and in its relative evolution in $0 < z < 2$. Some of the intrinsic problems that arise from the adoption of fixed calibration factors for the relation between SFR density and luminosity density can be partially addressed by computing the luminosity density explicitly from a model universe for comparison with observations (cf. Figure 1).

At first sight, the inconsistency between the SFR inferred from 200 nm and Hα calibrations could be regarded as a serious problem. However, the difference between the two values contains potentially useful diagnostic power regarding the star formation history. Observations of a variety of different diagnostics of the star formation rate in a sample of galaxies could provide a more robustly constrained star formation history, by allowing the determination of other important factors (such as type-specific IMFs). However, the number of star formation diagnostics accessible to observation is not large, and there are many parameters to be constrained. Clearly, the possible existence of type-specific IMFs and star-formation histories presents a significant challenge to any systematic investigation of the cosmic evolution of star formation.

We wish to thank Michael Rowan-Robinson for helpful comments and suggestions. JA gratefully acknowledges support in the form of a scholarship from the Science and Technology Foundation (FCT, Portugal) through Program Praxis XXI.

REFERENCES

Blain, A. W., Smail, I., Ivison, R. J., & Kneib, J.-P. 1999, MNRAS, 302, 632

Bressan, A., Fagotto, F., Bertelli, G., & Chiosi, C. 1993, A&AS, 100, 647

Connolly, A. J., Szalay, A. S., Dickinson, M., SubbaRao, M. U., & Brunner, R. J. 1997, ApJ, 486, L11

Cowie, L. L., Hu, E. M., Songaila, A., & Egami, E. 1997, ApJ, 481, L9

Cowie, L. L., Songaila, A., & Barger, A. J. 1999, AJ, 118, 603

Cram, L., Hopkins, A., Mobasher, B., & Rowan-Robinson, M. 1998, ApJ, 507, 155

Fioc, M., & Rocca-Volmerange, B. 1997, A&A, 326, 950

Flores, H., Hammer, F., Thuan, T. X., Césarsky, C., Desert, F. X., Omont, A., Lilly, S. J., Eales, S., Crampton, D., & Le Fèvre, O. 1999, ApJ, 517, 148

Gallego, J., Zamorano, J., Aragón-Salamanca, A., & Rego, M. 1995, ApJ, 455, L1

Glazebrook, K., Abraham, R., Santiago, B., Ellis, R., & Griffiths, R. 1998, MNRAS, 297, 885

Hughes, D., *et al.* 1998, Nature, 394, 241

Kennicutt, R. C., Jr. 1983, ApJ, 272, 54

Kennicutt, R. C., Jr., Tamblyn, P. & Congdon, C. E. 1994, ApJ, 435, 22

Leitherer, C., *et al.* 1996, PASP, 108, 996

Lilly, S. J., Le Fèvre, O., Hammer, F., & Crampton, D. 1996, ApJ, 460, L1

Madau, P., Ferguson, H. C., Dickinson, M. E., Giavalisco, M., Steidel, C. C., & Fruchter, A. 1996, MNRAS, 283, 1388

Madau, P., Pozzetti, L., & Dickinson, M. 1998, ApJ, 498, 106

Pascarelle, S. M., Lanzetta, K. M., & Fernández-Soto, A. 1998, ApJ, 508, L1

Pozzetti, L., Bruzual A., G., & Zamorani, G. 1996, MNRAS, 281, 953

Rowan-Robinson, M., *et al.* 1997, MNRAS, 289, 490

Schaerer, D. 1999, in Building Galaxies: from the Primordial Universe to the Present, ed F. Hammer, T. X. Thuân, V. Cayatte, B. Guiderdoni, & J. Tran Thanh Van (Gif-sur-Yvette: Editions Frontières), in press (astro-ph/9906014)

Sullivan, M., Treyer, M. A., Ellis, R. S., Bridges, T. J., Milliard, B., Donas, J. 1999, MNRAS, in press (astro-ph/9910104)

Tinsley, B. M., & Danly, L. 1980, ApJ, 242, 435

Tresse, L., & Maddox, S. J. 1998, ApJ, 495, 691

Treyer, M. A., Ellis, R. S., Milliard, B., Donas, J. & Bridges, T. J. 1998, MNRAS, 300, 303

This preprint was prepared with the AAS LaTeX macros v5.0.

Table 1. Calibration constants C^p

Galaxy type	C^{200} $M_\odot$ yr^{-1} / W Hz^{-1}	$C^{H\alpha}$ $M_\odot$ yr^{-1} / W
early	1.887×10^{-21}	3.381×10^{-34}
late	1.094×10^{-21}	1.176×10^{-34}

Table 2. Type-specific contributions to luminosity and SFR densities at $z = 0$

			200 nm		Hα	
Type	$\dot{\rho}_k$	%	log ($\mathcal{L}^{200}$)	%	log ($\mathcal{L}^{\mathrm{H}\alpha}$)	%
E/S0	0.0000	0	16.58	0	28.95	0
Sab-cd	0.0040	38	18.31	27	31.08	18
Scd-dm	0.0040	38	18.55	46	31.53	50
vB	0.0026	24	18.31	27	31.34	32
Total	0.0106	100	18.88	100	31.83	100

Note. — $\dot{\rho}_k$ in $\mathrm{M}_\odot$ yr^{-1} Mpc^{-3}, $\mathcal{L}^{200}$ in W Hz^{-1} Mpc^{-3} and $\mathcal{L}^{\mathrm{H}\alpha}$ in W Mpc^{-3}

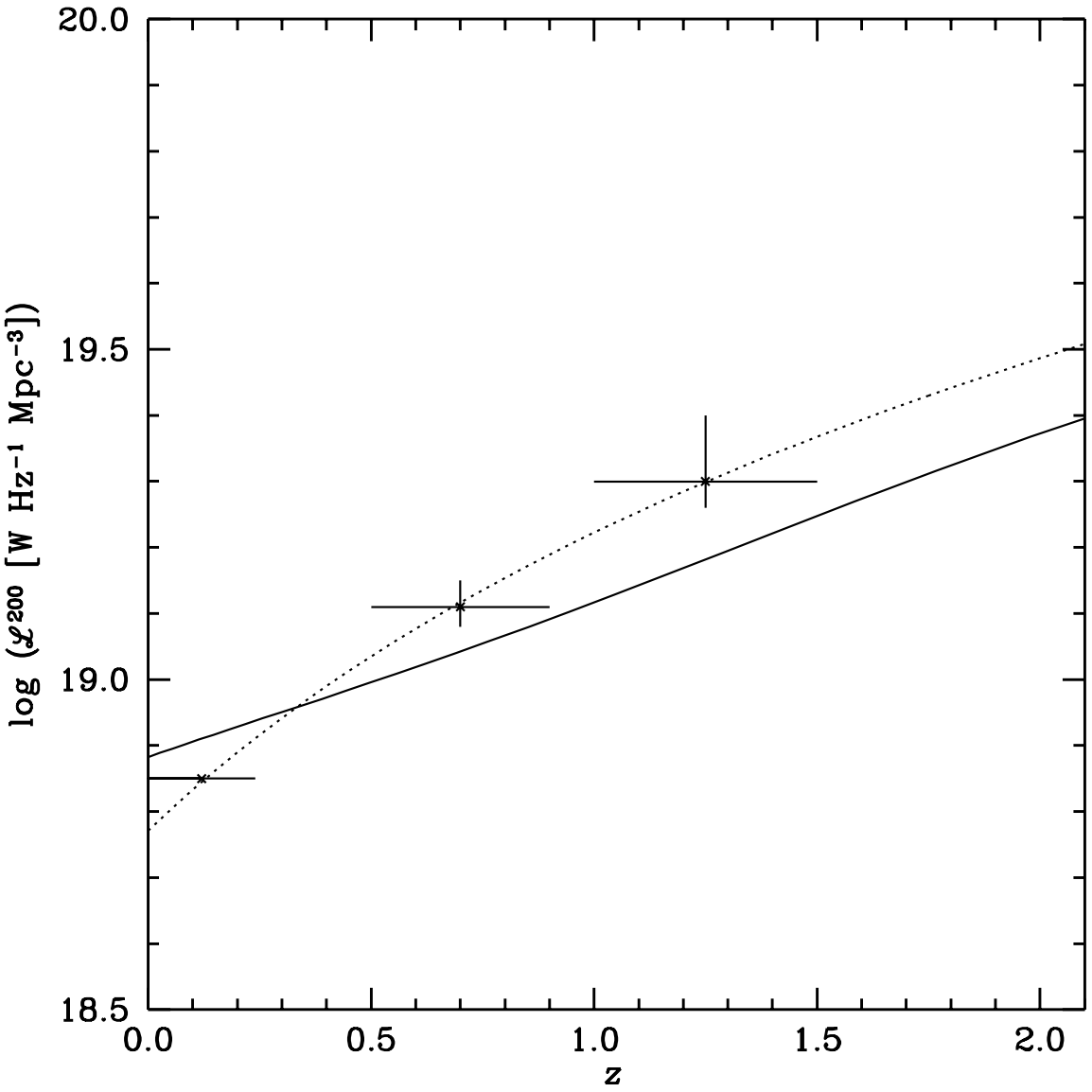

Fig. 1.— Rest frame 200 nm luminosity density predicted using the model universe (solid line), compared with the values measured by Cowie, Songaila & Barger (1999) (crosses) and fitted to a parametric form (dotted line). The measurements adopt $H_0 = 65$ km s^{-1} Mpc^{-1}. Conversion to the cosmology used in this paper would reduce the measured luminosity density by ≈ 0.4 dex but a correction for UV extinction would increase the value by a similar amount.

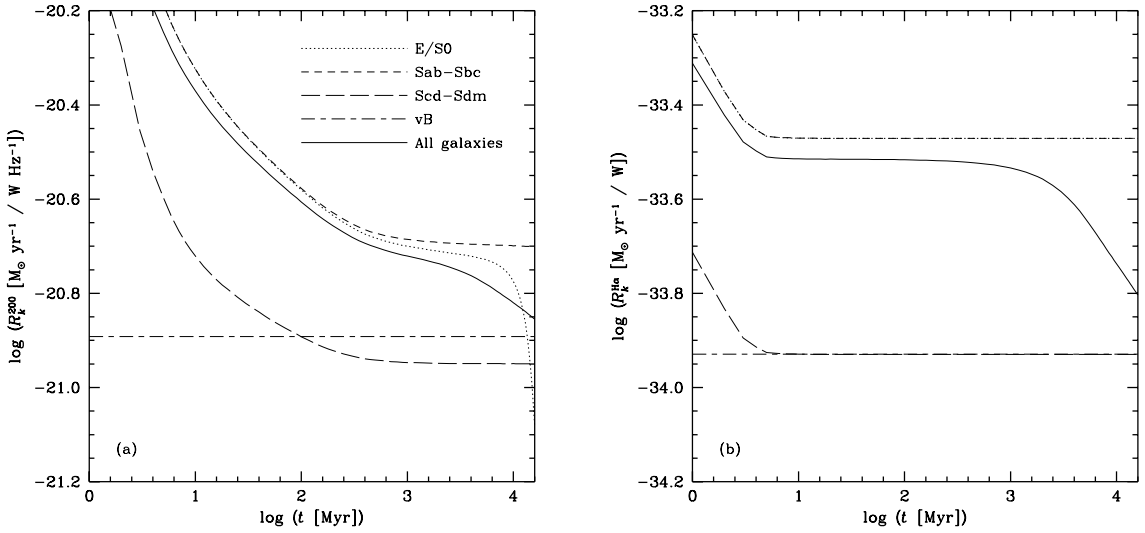

Fig. 2.— (a) The evolution with time of the ratio of SFR density to luminosity density at 200 nm for each galaxy type considered in this study. The solid line represents the evolution of the global ratio of the total star formation rate density to luminosity density, $R^{200}(t)$. (b) The same as (a), for Hα.

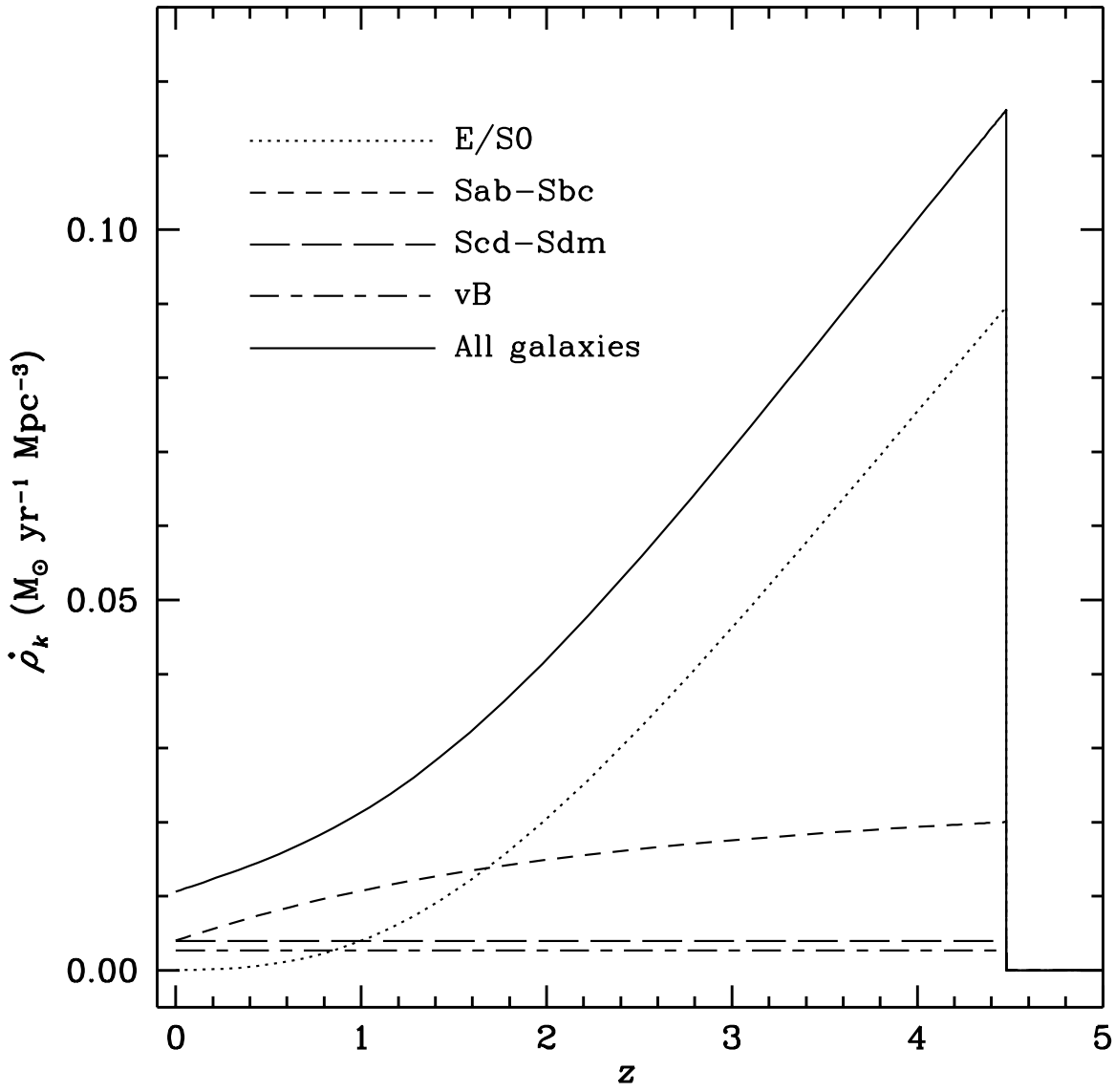

Fig. 3.— Evolution of the SFR density for the 4 galaxy types, derived using the parametric SFRs and luminosity functions of Pozzetti *et al.* The solid curve represents the global SFR density.

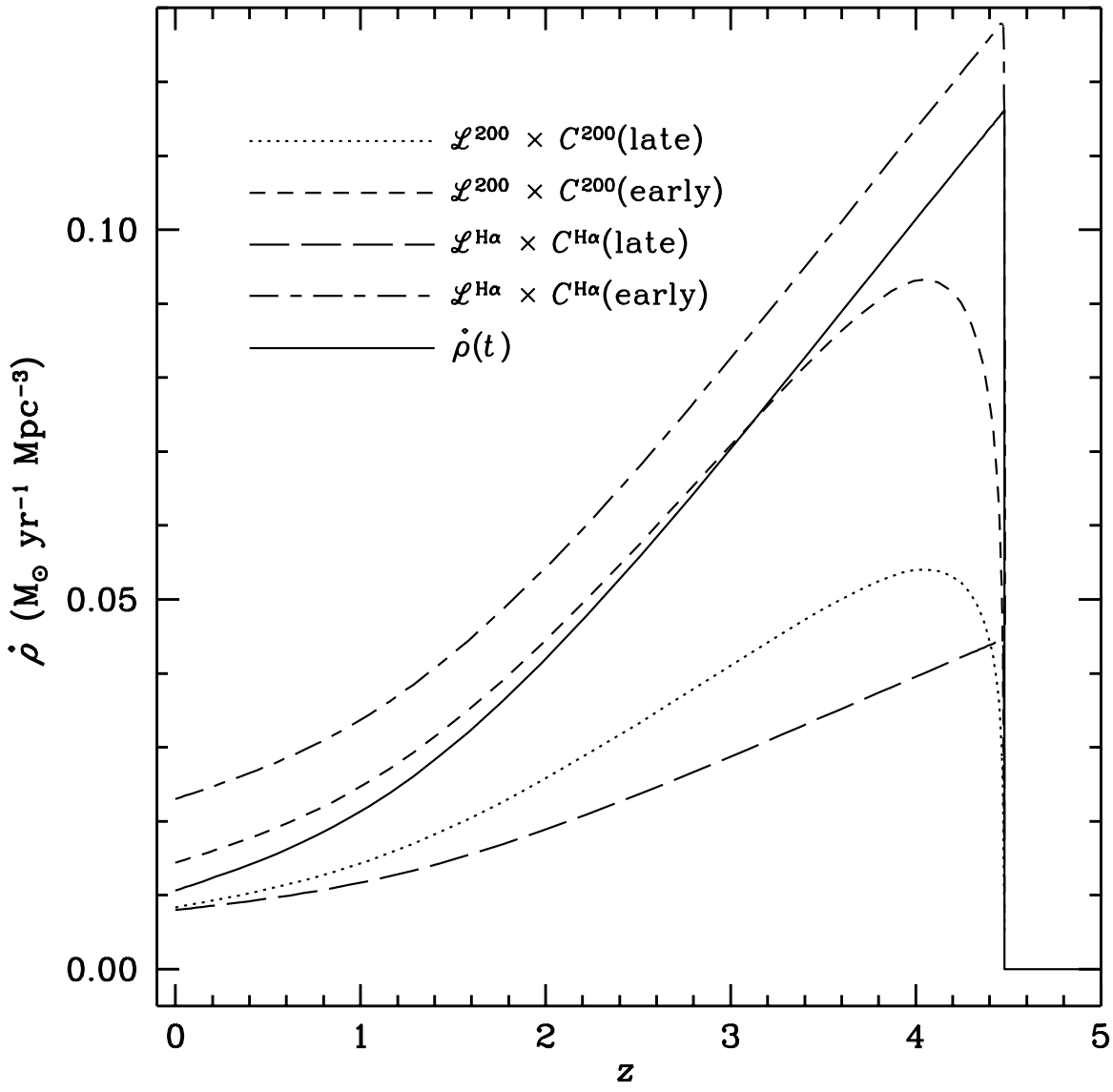

Fig. 4.— Evolution of the estimated global SFR density, using the calibrations derived as explained in the text (C^p) and listed in Table 1. There are calibrations for both Salpeter (late) and Scalo (early) IMFs. The solid curve is the actual global SFR density transferred from Fig. 3.